
This is an electronic reprint of the original article.
This reprint may differ from the original in pagination and typographic detail.

Zhang, Peize; De Guzman, Mar Francis; Li, Xuhong; Cai, Xuesong; Haneda, Katsuyuki; Tervo, Nuutti; Parssinen, Aarno; Tufvesson, Fredrik; Kyosti, Pekka

Understanding Subterahertz Radio Channels: The Impact of Beamforming on Wireless System Design

Published in:
IEEE Vehicular Technology Magazine

DOI:
[10.1109/MVT.2025.3573093](https://doi.org/10.1109/MVT.2025.3573093)

Published: 01/01/2025

Document Version
Publisher's PDF, also known as Version of record

Published under the following license:
CC BY

Please cite the original version:
Zhang, P., De Guzman, M. F., Li, X., Cai, X., Haneda, K., Tervo, N., Parssinen, A., Tufvesson, F., & Kyosti, P. (2025). Understanding Subterahertz Radio Channels: The Impact of Beamforming on Wireless System Design. *IEEE Vehicular Technology Magazine*, 20(3), 49-57. <https://doi.org/10.1109/MVT.2025.3573093>

This material is protected by copyright and other intellectual property rights, and duplication or sale of all or part of any of the repository collections is not permitted, except that material may be duplicated by you for your research use or educational purposes in electronic or print form. You must obtain permission for any other use. Electronic or print copies may not be offered, whether for sale or otherwise to anyone who is not an authorised user.



©SHUTTERSTOCK.COM/VIDEOFLOW

UNDERSTANDING SUBTERAHERTZ RADIO CHANNELS

The Impact of Beamforming on Wireless System Design

Peize Zhang^{ID}, Mar Francis De Guzman^{ID}, Xuhong Li^{ID}, Xuesong Cai^{ID}, Katsuyuki Haneda^{ID},
Nuutti Tervo^{ID}, Aarno Pärssinen^{ID}, Fredrik Tufvesson^{ID}, and Pekka Kyösti^{ID}

Wireless connectivity in the subterahertz (sub-THz) band, spanning from 100 GHz to 300 GHz, is envisioned as an enhanced feature of 6G and beyond. Due to significant propagation losses at these frequencies, the transmission of sub-THz signals relies heavily on high antenna directivity, realized by beamforming. In this article, we present a newly developed sub-THz stored channel model, and perform a realistic evaluation of the impact of beamforming on sub-THz link establishment and data transmission. Unlike the

propagation channel between the transmitting and receiving antennas, the radio channel is observed by a pair of beams. Incorporating the impact of beamforming into measured sub-THz propagation channel data enables to gain insights into the key factors that determine, among others, sub-THz beam alignment strategy and waveform design, ultimately enhancing spectral efficiency.

Introduction

Background and Motivation

The sub-THz band encompasses frequencies between 100 and 300 GHz and holds promising potential to

Digital Object Identifier 10.1109/MVT.2025.3573093

Date of publication 4 August 2025; date of current version 15 September 2025.

promote technological advancement in 6G and beyond [1]. The vast amount of spectrum serves up extreme data rates for densely located short radio links. The sub-THz band also raises the potential for very accurate localization and sensing using compact radios, which can be effectively deployed everywhere [2].

As propagation loss is one of the fundamental challenges facing sub-THz frequencies [3], both communication and sensing functionalities that operate at sub-THz frequencies rely on directional transmission. This not only increases the link budget with sufficient beamforming gains but also enables the suppression of multipaths and interference [4]. However, it imposes substantial technical challenges in beam management considering the usage of pencil beams at both link ends. Also, many existing studies have demonstrated that the use of highly directive beamforming or beam-steerable antennas results in pronounced differences in the observed channels compared to the use of omnidirectional antennas [4], [5], [6]. Thus, knowing the sub-THz channels while accounting for the impact of directional beams is critical for sub-THz wireless system design and optimization.

The *propagation channel* characterizes how the signals propagate from the transmitting (Tx) antenna to the receiving (Rx) antenna and how they interact with the objects in the environments. For wireless systems that make use of higher frequencies, e.g., sub-THz, the corresponding propagation channel models must be first upgraded as the fundamental propagation effects are, to some extent, different from those below 100 GHz [3], [6]. Furthermore, a deeper understanding of the underlying *radio channel*—the channel observed through specific antennas or beams—is essential for wireless system design because the system operates in the radio channel rather than the propagation channel, particularly when utilizing analog or hybrid beamforming architectures. Although sub-THz channel measurement data have traditionally been used for propagation channel modeling, antenna patterns are typically de-embedded from the measured channel impulse responses (CIRs) via preprocessing. However, this article focuses on radio channel characterization, i.e., including the impact of antennas and beamforming in the estimated propagation paths through postprocessing, thereby drawing design insights from such analysis.

System Design Aspects

Given the configurations of a sub-THz wireless system, such as carrier frequency, bandwidth, Tx power, modulation and coding scheme, and Rx noise figure, its coverage range is fundamentally determined by path loss and antenna array gains (which increase with the number of elements). Although molecular absorption contributes to path loss, it can be neglected for carefully selected

frequency bands and short link distances. A detailed sub-THz link budget analysis is presented in [7] and field trials in [6]. Thus, the main objective of this study is to derive design insights from an empirical analysis of the space-time characteristics of the sub-THz radio channel.

For the communication-only service, the first step is to establish an initial physical link between the base station (BS) and the user equipment (UE) through beam alignment, which incurs high training overhead when adjusting the narrow beams at sub-THz frequencies. This gets worse for fast time-varying channels because the beam training results become outdated quickly. One solution is to leverage out-of-band channel information if the system operates across multiple carrier frequencies [8] or uses a so-called non-stand-alone mode. The integration of sensing capabilities within a communication system offers another solution, where side information from, e.g., radio-based sensing, can guide beam alignment and avoid extensive (blind) beam training. However, depending on the level of integration of sensing and communications in hardware, frequency, waveform, and so on, the side information requires further processing to ensure precise alignment of beams. The success of these solutions, particularly in employing low-complexity methods to fully reuse this information, depends heavily on the spatial channel similarity either between different frequency bands or within the same band (i.e., in-band operation) but for different services. After the initial process of beam establishment, sub-THz systems will steer the Tx and Rx beams and continue to track the beam directions to maintain the link. The beam tracking process faces similar challenges when exploiting out-of-band or in-band radio channel information.

In the connected state, the design of sub-THz transmission waveforms and Rx equalizers must also take into account the system's underlying radio channel. In [4], single-carrier modulation, with a simple equalizer or even without one, is recommended for the early deployment of sub-THz systems. This is experimentally validated only in a simple indoor line-of-sight (LOS) scenario using horn antennas with fixed half-power beamwidths (HPBW). Based on more extensive measurement campaigns, the required number of equalizer taps varies depending on channel conditions such as environment and Tx-Rx location as delay dispersion parameters are highly sensitive to these factors [6]. For sub-THz multi-carrier modulation based on orthogonal frequency-division multiplexing with cyclic prefix (CP), the CP length should be greater than the delay spread (DS) or maximum excess delay (MED) of the multipath channel to mitigate both intersymbol and intercarrier interference. It is anticipated that the DS and MED could be significantly reduced when the propagation paths are weighted by steered beam patterns. Therefore, it is necessary to quantitatively investigate the impact of directive beams

on the time dispersion characteristics of sub-THz channels and assess how the system can benefit from such analysis to improve its spectral efficiency.

This article first presents a sub-THz stored channel model that was recently developed in European 6G flagship projects Hexa-X and Hexa-X-II, and which incorporates the impact of different beam patterns in propagation paths via postprocessing. Using this model and the associated data, some insights for sub-THz wireless system design can then be drawn. Finally, we discuss the future directions in sub-THz radio channel characterization and its applications.

Sub-THz Stored Channel Model

Framework

The framework used for developing the sub-THz stored channel model is shown in Figure 1. The propagation channel data at 140 GHz was collected using a vector network analyzer-based channel sounder with an omnidirectional antenna fixed on the Tx side and a horn antenna rotating in the azimuth plane on the Rx side. Indoor propagation channel data were collected in an entrance hall, while outdoor measurements were conducted in three environments: a suburban area, a residential area, and a city center. Further details on the measurement configurations and environments can be found in [9]. The CIRs can be obtained by performing an inverse fast Fourier transform of measured channel frequency responses. Preprocessing of the single-directional CIRs results in estimated multipath components (MPCs) with enhanced angular resolution (i.e., 1°) while de-embedding the antenna patterns. Each MPC is characterized by its path gain, propagation delay, and azimuth angle of arrival (AoA). To obtain bidirectional channel information while avoiding mechanical rotation of antennas at both link ends, a measurement-based ray launcher (MBRL) was employed, where the MBRL only searches for the rays at given angular intervals that are determined by the estimated AoAs. Apart from the additional path information, e.g., azimuth

angle of departure, elevation angle of departure, and elevation AoA, major wave-interacting objects at the channel sounding sites are identified, including the types and coordinates of the first- and last-bounce scatterers. Understanding wave-interacting objects is crucial for evaluating localization and sensing. This information, together with the coordinates of the Tx and the Rx, can be stored and played back.

The impact of antennas or beamforming is included via postprocessing, which is the final step in Figure 1. The predefined antenna geometries and beam patterns as well as their orientations can be integrated into the playback of the propagation channel MPCs. The MATLAB implementation of the sub-THz stored channel model with the measurement data in one indoor and three outdoor environments, containing more than 200 links in both LOS and non-line-of-sight (NLOS) scenarios, is available at [9].

Human Blockage

The sub-THz propagation channel data used to develop the stored channel model were collected under static condition, with both the antennas and the surrounding environment remaining unchanged. To partially account for mobility in the proposed model, moving scatterers are introduced into the propagation environment through postprocessing. Specifically, a measured attenuation pattern caused by a moving human blockage at the channel sounding frequency (i.e., 140 GHz) was incorporated. Figure 2 gives an example of measured human blockage attenuation patterns against elapsed time. Here, two cases are considered where a human blocker in frontal or lateral orientation is crossing the LOS link between the Tx and the Rx at a constant speed of 1 m/s. The simulation result based on the double knife-edge diffraction model fits well with the measurement result for the frontal crossing case. Figure 2 shows that human blockage at 140 GHz can cause deep fades of more than 30 dB, with attenuation levels depending on the physical dimensions of the human body and the faced direction, i.e., frontal or lateral orientation of the blocker while

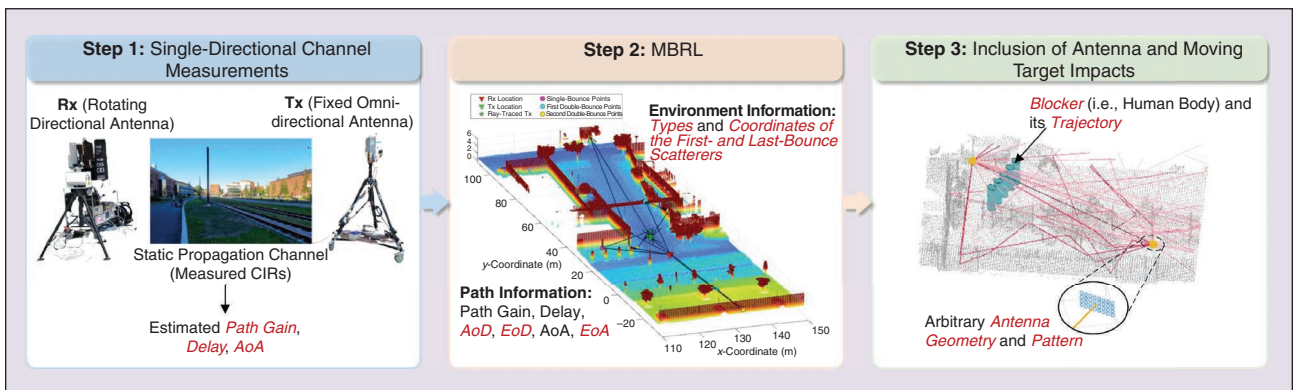


FIGURE 1 The framework of the sub-THz stored channel model. AoA: angle of arrival; AoD: azimuth angle of departure; EoD: elevation angle of departure; EoA: elevation angle of arrival; MBRL: measurement-based ray launcher.

crossing the link. Negative attenuation values appear due to diffraction gains when the human blocker moves close to the direct path between the Tx and the Rx.

When integrating the measured attenuation pattern into the stored channel model, we first define the trajectory, velocity, and orientation of the moving human body in the environment of the model. As depicted in Figure 1, the human body is simplified as a blue elliptical cylinder. A blockage event on the individual path is triggered according to the position of the human blocker, i.e., identification of the interaction points of the blocker and the propagation paths. The attenuation of the individual path is determined geometrically. As the results in Figure 2 were measured with a blocker moving at a constant speed of 1 m/s, the attenuation patterns will be scaled according to the predefined velocity of the moving human body. To account for variations in body size and clothing, corresponding attenuation patterns must be measured separately.

Near-Field Extension

The extracted MPCs from the second step are valid only under the far-field condition for both Tx and Rx antennas. However, when using electrically large antenna arrays and

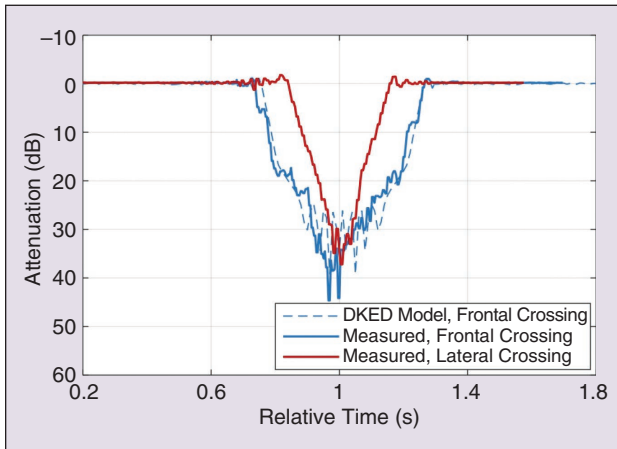


FIGURE 2 An example of measured attenuation pattern caused by human blockage at 140 GHz. DKED: double knife-edge diffraction.

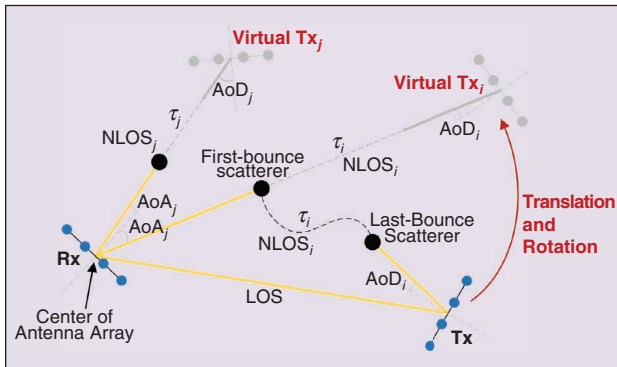


FIGURE 3 An illustration of the near-field extension of the stored channel models.

having short link distances, the far-field condition of emanating fields from the antenna array may not be fulfilled. As a result, received wavefronts may be nonplanar and, in the extreme case, antenna elements may even experience different shadowing due to close-by obstacles. The former effect, i.e., spherical (or other curved) wavefronts, can impact beamforming performance, especially in the null directions of steered beams. Therefore, enabling near-field channel simulation in the proposed sub-THz stored channel model would be beneficial.

Spherical wavefronts can be modeled for an LoS path by knowing the coordinates of Rx and Tx antenna elements, calculating the distance between all Rx/Tx antenna pairs, and determining phase offsets between array elements based on these distances at considered frequencies. If either end of the link is moving, the distance increment per time instant can be determined as well, and frequency-dependent Doppler shifts can be obtained by the same principle.

For NLOS paths, wave curvature modeling is not that trivial as it depends on the wave-object interaction types and distances between interacting objects. Assuming specular reflections, virtual locations of, e.g., Tx array elements can be determined and antenna pair distances calculated as with the LOS path for the virtual anchors. Translation and rotation of the Tx array to a virtual position are performed for each path, as shown in Figure 3, and so spherical wavefronts and frequency-dependent Doppler can be modeled. This procedure is applicable not only with the stored channel model but also with any geometric model, as far as path angles and propagation delays are known.

Design Guidelines for Sub-THz Wireless Systems

Using the sub-THz stored channel model and the associated indoor and outdoor measurement data [9], some guidelines can be drawn for sub-THz wireless system design.

Number of Relevant Beams

Instead of employing arbitrarily oriented beam patterns in the sub-THz multipath channels, the potential beam pointing directions used for data transmission need to first be identified. Such a process, similar to blind beam training where the BS performs beam sweeping within a specified angular range and selects a set of Tx/Rx beams [see Figure 4(a)], is realized via two steps. We first perform a circular convolution of the steered beam pattern and the power angular spectrum (PAS) of the propagation channel, resulting in a *beamformed channel*, and then detect the local maxima of the beamformed PAS. As shown in Figure 4(b), the black circles represent the MPCs of the propagation channel specified by the stored model. Five beam directions (red squares) with power levels within 10 dB of the maximum power can be detected from the PAS of the beamformed channel. This narrow dynamic range of beam powers is chosen because the dynamic range

of sub-THz radio transceivers is typically limited, particularly at high bandwidths. In this example, the beam pattern of an eight-element half-wavelength-spaced uniform linear array (ULA) is used for beam sweeping over the entire $[0^\circ, 360^\circ]$ space. Note that the beam pattern is defined only over the boresight half plane, while the gain is set to a constant value of -60 dB for the back half plane. Despite the high front-to-back ratio of the antenna array, this has a minimal effect on the results, which are primarily dominated by the main lobe.

Although there are several significant paths in a sub-THz link, the number of separable beams is much smaller. For phased-array-based sub-THz systems, the derived number of beams from beamformed channels is seen as the practical upper limit of the number of independent beams, given the aperture size of the antenna array, i.e., beamwidth. Figure 5 shows the average number of beams estimated from beamformed channels across different scenarios. Beam patterns of half-wavelength-spaced ULAs with four, eight, 16, and 32 elements are used, corresponding to the HPBWs of 26.3° , 12.8° , 6.4° , and 3.2° , respectively. The number of estimated beams reduces with increasing HPBW of the beam pattern. Most sub-THz indoor LOS and outdoor links support only one to two independent beams for data transmission, even if there are a number of resolvable MPCs in the propagation channel. However, indoor NLOS links show more beam directions than other links because the power of NLOS MPCs is distributed over the 2π azimuth plane rather than concentrated along the direction of the LOS components. Sub-THz transceivers could be designed to support multiple simultaneous beams.

Out-of-Band and In-Band Beamformed Channel Similarity

The success of side-information-aided sub-THz beam alignment and tracking schemes strongly depends on the similarity of the beamformed channels observed by co-located radio systems using different hardware and/or frequencies. The estimated beam direction information from the co-located communication systems or radio-based sensing systems can be shared to establish and maintain sub-THz highly directional links with greatly reduced overhead. With the practical constraints set by the radio-frequency (RF) hardware, these systems operating in the same or different frequency bands will probably utilize different antenna geometries and beamforming architectures, leading to different beam patterns. In this sense, rather than bluntly comparing the PASs of beamformed channels observed by different beam patterns, we may use a beam direction-based metric for measuring beamformed channel similarity. This is performed by first estimating potential beam directions from beamformed channels, and then calculating the summed power of the beamformed PAS at beam directions estimated across different frequencies and (or)

beam patterns. Their power ratio, or its inverse (i.e., the power loss), quantifies the degradation caused by using side information from either out-of-band or in-band channels only [10]. A smaller power ratio indicates lower

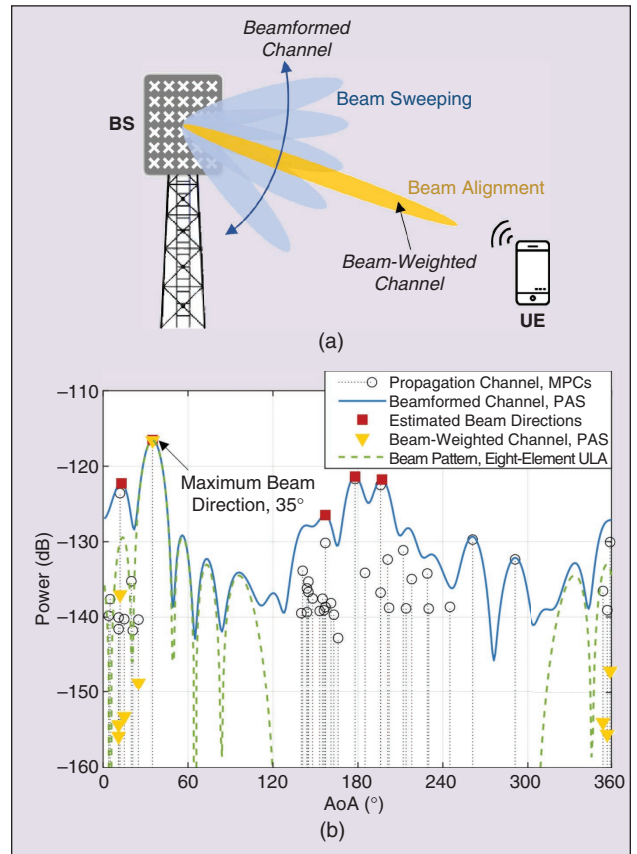


FIGURE 4 A comparison of propagation, beamformed, and beam-weighted channels. (a) An illustration of BS beams. (b) An example of measured propagation paths in angular domain, beamformed PAS, beamweighted propagation paths, and estimated beam directions. PAS: power angular spectrum; ULA: uniform linear array.

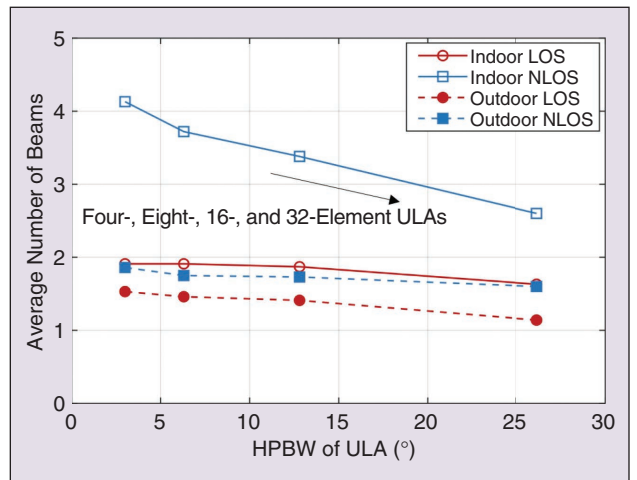


FIGURE 5 The average number of beams estimated from single-directional beamformed channels using the beam patterns of four-, eight-, 16-, and 32-element ULAs on the Rx side.

channel similarity. We do not directly compare the differences in beam pointing angles as even small angle deviations can result in significant power degradation for sub-THz pencil beamforming.

In [10], we analyzed the beam direction-based beamformed channel similarity based on ray-tracing simulated data across five frequencies below 100 GHz. The statistical results over thousands of Tx-Rx links show that the degree of spatial or beam direction-based similarity of the beamformed channels observed by the low- and high-band systems is related to the antenna's beamwidth, frequency gap, and link conditions. The higher the spatial similarity level of the beamformed channels, the more accurate beam information can be provided by the lower-frequency beamformed channel for higher-frequency beam alignment and tracking. Once multiband channel data at identical Tx-Rx settings become available, we can promote a feasibility study of sub-THz link configuration using out-of-band spatial channel information.

Sub-THz communication and radar sensing systems are expected to provide both functionalities simultaneously at the same frequency, i.e., in-band operation, while sharing potentially most of the hardware. One possible solution is to consider a multibeam design, which forms separate controllable beams for communications and radar sensing [11], [12]. Thus, we propose comparing the beam direction-based similarity of in-band beamformed channels, introduced by using separate communication and radar sensing beams with different HPBWs. For simplicity, ideal 3rd Generation Partnership Project (3GPP) beam patterns (i.e., no sidelobes) that have different HPBWs [10] are employed for communications and sensing services. Figure 6 compares the cumulative distribution functions of the power ratio using sub-THz indoor LOS and NLOS channel data in the stored channel model [9]. When the

HPBW of the radar sensing beam $\phi_{3dB,radar}$ is larger than that of the communication beam $\phi_{3dB,com}$, the figure shows a much higher power loss (i.e., the inverse of power ratio) compared with the case of $\phi_{3dB,radar} < \phi_{3dB,com}$. Moreover, a slightly more severe power loss can be observed in the indoor NLOS scenario due to more potential beam directions, as shown in Figure 5. The very low power loss clearly shown in Figure 6 means a high level of in-band beamformed channel similarity. Thus, sub-THz in-band sensing channel information, i.e., estimated beam directions, can be directly utilized to align communication beams, even though beams with small differences in HPBW, such as 5° and 10°, observe distinct beamformed channels.

In brief, both out-of-band information from lower-frequency communication channels and in-band information from radar sensing channels can assist in guiding beam alignment, but the process cannot rely on it solely. The angular resolutions of the antenna arrays involved should not exhibit significant discrepancies.

Delay Dispersion of Beam-Weighted Channel

Once the potential beam directions have been determined, the BS and the UE will steer Tx or Rx beams to these directions. As shown in Figure 4(b), the beam pattern of eight-element ULAs (green dashed line) is steered to the direction of 35° having maximum beam power, i.e., the *max beam* case. The MPCs of the propagation channel are weighted by the corresponding beam pattern, resulting in a *beam-weighted channel*. This process is similar to spatial filtering, where the propagation paths from other directions are suppressed [see the downward-pointing triangles in Figure 4(b)]. It becomes evident that the values of time dispersion parameters such as DS and MED will be significantly reduced compared to those of the propagation channel. As the CP length is related to the DS σ_τ or MED τ_{MED} of beam-weighted channels, such a reduction leads to further improvement in spectral efficiency by optimizing the CP length.

For conceptual simplicity, we perform beamforming only at the Rx side, and the beam pattern of eight-element half-wavelength-spaced ULAs is employed in the sub-THz stored channel model where, for each Tx-Rx link, the beam is always steered to the maximum beam direction. However, the same postprocessing methods can also be extended and applied for bidirectional beamforming using arbitrary beam patterns. Table 1 lists the statistics of the DS and MED of the beam-weighted and

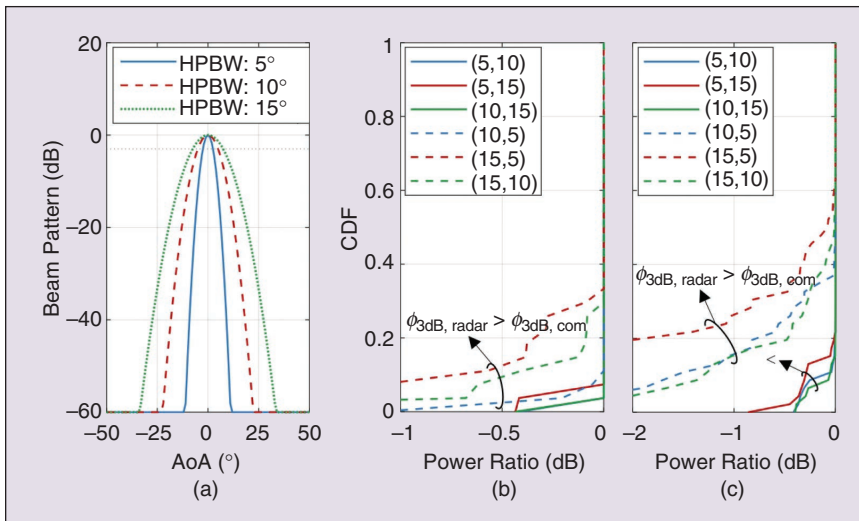


FIGURE 6 3GPP beam patterns with different HPBWs, such as 5°, 10°, and 15, and the empirical cumulative distribution functions (CDFs) of the power ratio when using in-band sensing channel information for communication beam alignment. (a) 3GPP beams. (b) LOS. (c) NLOS.

propagation channels, respectively. The mean values of the DS and MED of the propagation channel become less than halved after filtering by the 12.8° HPBW beam pattern of eight-element ULAs. For the beam-weighted channel, the median values of the time dispersion parameters are lower than their mean values. This is because, for most Tx–Rx links, there are very few paths whose beam-weighted path gains fall within the 30-dB dynamic range when calculating DS and MED. And these paths are more concentrated in both the time and angular domains. For indoor environments, both delay dispersion parameters of NLOS links can take on much higher values than those of LOS links, while an opposite trend can be observed for outdoor environments.

To investigate the impact of HPBW on delay dispersion characterization, we switch back to using 3GPP beam patterns, which can provide finer HPBW granularity. Both delay dispersion parameters (see Figure 7) increase significantly with increasing HPBW in the range of [2°, 15°]. Here, we do not distinguish the results for indoor/outdoor LOS/NLOS links. The 90th percentiles of σ_τ and τ_{MED} , i.e., 90% of all cases falling below these values, do not show a continuous increase when much wider beam patterns are used. In addition, even though the propagation channels are weighted by a very narrow beam, e.g., with an HPBW of 6°, the average 90 percentiles of σ_τ and τ_{MED} still take very high values, i.e., 14.71 and 162.84 ns, respectively. For links within extremely low σ_τ and τ_{MED} values (e.g., zero), this occurs because only a single path has a beam-weighted path gain within the 30-dB power threshold when calculating delay dispersion parameters.

In summary, the delay dispersion of the beam-weighted radio channel is strongly affected by beamforming and varies with propagation scenario. Meanwhile, the expected antenna beamwidth should be a key consideration in sub-THz system design because it can lead to an improvement in spectral efficiency through optimized length of the CP or the equalizer.

Future Research Directions

Hardware Impairment-Aware Channel Modeling

In this article, the radio channel characteristic is looked at from the perspective of ideal beam patterns. However, in reality, the radio channel is looked at through the lens of sub-THz hardware, including antennas, sub-THz front-end components, and the rest of the RF chain. In particular, antenna element beam patterns and power amplifiers, in

TABLE 1 Statistics of the maximum beam DS and MED in different scenarios using the beam pattern of eight-element ULAs.

Environment	Scenario	Parameters (ns)	Beam-Weighted Channel			Propagation
			Mean	Median	p90*	Mean
Indoor	LOS	σ_τ	3.5	2.39	7.19	11.54
		τ_{MED}	57.55	40.12	137.78	119.1
	NLOS	σ_τ	10	4.11	35.76	26.38
		τ_{MED}	74.1	52.9	185.24	166.28
Outdoor	LOS	σ_τ	11.59	2.49	32.91	23.3
		τ_{MED}	115.57	16.31	341.64	246.04
	NLOS	σ_τ	9.41	2.04	29.37	29.82
		τ_{MED}	33.08	5.33	95.43	159.13

*p90: 90th percentile of the σ_τ or τ_{MED} .

addition to their interconnects, may significantly vary from antenna to antenna. Especially in systems that rely on analog beamforming, this variation cannot be completely calibrated, so they can have a noticeable impact on the array beam patterns and the observed radio channel [13]. Consequently, a general sub-THz radio channel model must explicitly incorporate the effects of hardware impairments introduced by real-world components. The development of impairment-aware channel models that reflect the interplay of RF nonidealities, antenna coupling, and propagation channels enables a more accurate evaluation of sub-THz system performance under realistic conditions. This in turn provides deeper insights into beam alignment, equalization optimization, and signal processing.

Sub-THz Dynamic Channel Sounding

The results and analysis presented earlier are based on static sub-THz channel data as most existing sub-THz

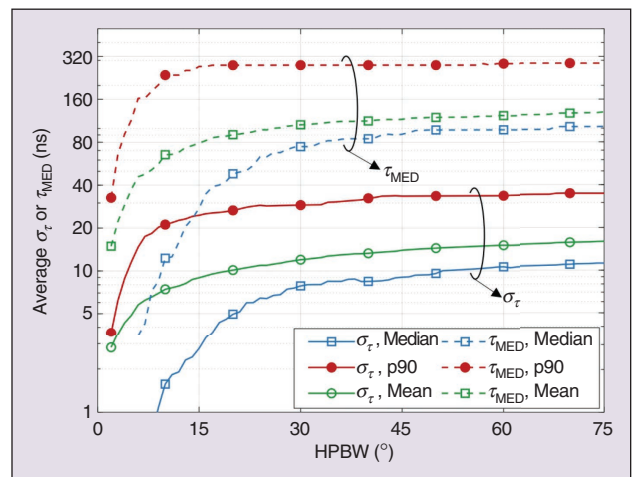


FIGURE 7 For the maximum beam case, average the DS and MED versus the HPBWs of the 3GPP beam patterns.

bidirectional channel sounding activities rely on the mechanical rotation of directional antennas at both link ends [3]. This approach leads to very slow measurements; bidirectional measurements typically need a few hours for a single link. A promising solution for enabling dynamic sub-THz channel sounding is the use of rotating mirrors. Instead of rotating antennas themselves, the Tx and Rx beams are oriented via rotating mirrors that reflect the incident signals from and to the fixed antennas, respectively. Recently developed rotating mirror-based sounders for millimeter-wave channel measurements can complete a full bidirectional azimuth scan within 1 s by precisely adjusting the mirror rotation speed [14]. Following this concept, it is feasible to upgrade such sounders for dynamic sub-THz channel measurements and characterization.

Beamformed Power Constraint

In the “[Design Guidelines for Sub-THz Wireless Systems](#)” section, we employ normalized beam patterns with varying HPBWs to form the radio channels, defined solely for the front half plane only, while setting beam gains for the back half plane to a constant value of -60 dB. However, practical constraints on beamformed power arise as well for radio systems that operate at different frequencies and serve diverse functionalities. By default, the corresponding Tx/Rx beam pattern gains are dictated by system specifications and application requirements. These factors primarily influence beam direction finding, where high-gain beams result in a greater number of potential beam pointing directions estimated from beamformed channels. Consequently, beam direction-based channel similarity must be reevaluated, considering both the width and gain of the sweeping beam.

Radio-Based Localization and Sensing

The aforementioned new characteristics of high-frequency channels and beam-based systems provide both inspiration and challenges for the design of sub-THz-based localization and sensing solutions. The use of large signal bandwidths and large antenna arrays greatly improves spatial resolution and thus sensing capabilities [2]. In the previous works [15], it was preliminarily shown that localization or simultaneous localization and mapping using high-frequency radio systems has the potential to deliver centimeter-level localization accuracy and mapping accuracy even in dynamic environments with strong multipath propagation, such as urban canyons and indoor environments. This can greatly facilitate both beam alignment and beam tracking. However, the narrow beamwidths that are formed with large arrays may lead to beam misalignment and therefore loss of target tracking, especially in highly dynamic scenarios. Beamwidth design should be adaptive according to specific applications and scenarios.

Conclusion

A deep understanding of radio channels is essential for the effective design of sub-THz wireless systems as different antennas or beams will modify the propagation channel and yield varying radio channels. In this work, we introduced a sub-THz stored channel model that can assist in incorporating the beamforming impact—more specifically, the impact of beam patterns—into field-measured MPCs of propagation channels. Two types of radio channels were defined: the *beamformed channel*, observed by continuously steered beams, being continuous in the angular domain and enabling the estimation of potential beam alignment directions, and the *beam-weighted channel*, which is constituted by one or a few beams steered to discrete directions, being more relevant to the data transmission phase.

Our measurements and analysis indicate that although sub-THz channels have a number of resolvable MPCs, the number of beams that they can support is typically limited to one to two for most of the indoor and outdoor links, except for the indoor NLOS case. The high spatial similarity level of out-of-band or in-band beamformed channels, given the practical constraints on beam patterns for different frequencies or services, facilitates rapid sub-THz link establishment by only exploiting beam orientation information. Sub-THz waveform and equalizer design is directly tied to the delay dispersion characteristics of beam-weighted channels. Our results further indicate that the delay dispersion is highly dependent on deployment scenarios and the beamwidth of steerable beamforming antennas. Future research directions were proposed to, among other things, investigate the dynamic characteristics of radio channels in the presence of hardware impairments for optimal sub-THz wireless system design.

Acknowledgment

This work was partly supported by the Hexa-X-II project, receiving funding from the Smart Networks and Services Joint Undertaking under the European Union’s Horizon Europe Research and Innovation Programme (Grant agreement 101095759), and partly by the Research Council of Finland (formerly the Academy of Finland) project (Grant number 348980) and the 6G Flagship Program (Grant number 346208).

Author Information



Peize Zhang (p.zhang@qub.ac.uk) is currently a lecturer (assistant professor) with the Centre for Wireless Innovation, Queen’s University, BT3 9DT Belfast, U.K. His research interests focus on propagation, deployment, and performance issues of millimeter-wave/terahertz communication systems. He is a Member of IEEE.



Mar Francis De Guzman (francis.deguzman@aalto.fi) is currently pursuing his D.Sc. degree in electrical engineering at Aalto University, 02150 Espoo, Finland. His research interests include radio channel measurements, simulations, and modeling for 6G wireless communication systems. He is a Member of IEEE.



Xuhong Li (xuhong.li@eit.lth.se) is a postdoctoral researcher in the Department of Electrical and Information Technology, Lund University, 22363 Lund, Sweden. Her research interests include radio-based localization and estimation of radio channels.



Xuesong Cai (xuesong.cai@pku.edu.cn) is an associate professor (and full research professor) at the School of Electronics, Peking University, Beijing 100871, China. His research interests include radio channel characterization, high-resolution parameter estimation, over-the-air testing, resource optimization, and radio-based localization for 5G/beyond 5G wireless systems. He is a Senior Member of IEEE.



Katsuyuki Haneda (katsuyuki.haneda@aalto.fi) is an associate professor with Aalto University, 02150 Espoo, Finland. His current research interests include radio-frequency instrumentation, measurements and modeling, millimeter-wave and terahertz radios, in-band full-duplex radio technology, and radio applications in medical and health-care scenarios. He is a Member of IEEE.



Nuutti Tervo (nuutti.tervo@oulu.fi) is an assistant professor (tenure track) with the Centre for Wireless Communications, University of Oulu, 90570 Oulu, Finland. His current research interests include radio-frequency transceivers, radio channel modeling, signal processing, and system-level analysis. He is a Member of IEEE.



Aarno Pärssinen (aarno.parssinen@oulu.fi) is with the Centre for Wireless Communications, University of Oulu, 90570 Oulu, Finland, where he is currently a professor leading devices and circuits research in the 6G Flagship program. His research interests include wireless systems, integrated circuitry, and transceiver architectures. He is a Fellow of IEEE.



Fredrik Tufvesson (fredrik.tufvesson@eit.lth.se) is a professor of radio systems with Lund University, 22363 Lund, Sweden. His research interest is the interplay between the radio channel and the rest of the communication system with various

applications in 5G/beyond 5G systems, such as massive multiple-input/multiple-output, millimeter-wave communication, vehicular communication, and radio-based positioning. He is a Fellow of IEEE.



Pekka Kyösti (pekka.kyosti@oulu.fi) is a research director with the 6G Flagship program and an adjunct professor with the Centre for Wireless Communications, University of Oulu, 90570 Oulu, Finland, and a senior specialist with Keysight Technologies. His research interests include radio channel characterization for 6G systems.

References

- [1] A. Shafiq, N. Yang, C. Han, J. M. Jornet, M. Juntti, and T. Kürner, "Terahertz communications for 6G and beyond wireless networks: Challenges, key advancements, and opportunities," *IEEE Netw.*, vol. 37, no. 3, pp. 162–169, May/June 2023, doi: [10.1109/MNET.118.2200057](https://doi.org/10.1109/MNET.118.2200057).
- [2] H. Chen, H. Sarrieddeen, T. Ballal, H. Wymeersch, M.-S. Alouini, and T. Y. Al-Naffouri, "A tutorial on terahertz-band localization for 6G communication systems," *IEEE Commun. Surveys Tuts.*, vol. 24, no. 3, pp. 1780–1815, 3rd Quart. 2022, doi: [10.1109/COMST.2022.3178209](https://doi.org/10.1109/COMST.2022.3178209).
- [3] C. Han et al., "Terahertz wireless channels: A holistic survey on measurement, modeling, and analysis," *IEEE Commun. Surveys Tuts.*, vol. 24, no. 3, pp. 1670–1707, 3rd Quart. 2022, doi: [10.1109/COMST.2022.3182539](https://doi.org/10.1109/COMST.2022.3182539).
- [4] L. Miretti et al., "Little or no equalization is needed in energy-efficient sub-THz mobile access," *IEEE Commun. Mag.*, vol. 62, no. 2, pp. 94–100, Feb. 2024, doi: [10.1109/MCOM.001.2200464](https://doi.org/10.1109/MCOM.001.2200464).
- [5] R. Piesiewicz, M. Jacob, M. Koch, J. Schoebel, and T. Kürner, "Performance analysis of future multigigabit wireless communication systems at THz frequencies with highly directive antennas in realistic indoor environments," *IEEE J. Sel. Topics Quantum Electron.*, vol. 14, no. 2, pp. 421–430, Mar./Apr. 2008, doi: [10.1109/JSTQE.2007.910984](https://doi.org/10.1109/JSTQE.2007.910984).
- [6] A. F. Molisch, J. Gomez-Ponce, N. Abbasi, W. Choi, G. Xu, and C. J. Zhang, "Properties of sub-THz propagation channels and their impact on system behavior: Channel measurements and transmission experiments," *IEEE Wireless Commun.*, vol. 31, no. 1, pp. 18–24, Feb. 2024, doi: [10.1109/MWC.001.2300329](https://doi.org/10.1109/MWC.001.2300329).
- [7] K. Rikkinen, P. Kyösti, M. E. Leinonen, M. Berg, and A. Pärssinen, "THz radio communication: Link budget analysis toward 6G," *IEEE Commun. Mag.*, vol. 58, no. 11, pp. 22–27, Nov. 2020, doi: [10.1109/MCOM.001.2000310](https://doi.org/10.1109/MCOM.001.2000310).
- [8] A. Ali, N. González-Prelcic, and R. W. Heath, "Millimeter wave beam-selection using out-of-band spatial information," *IEEE Trans. Wireless Commun.*, vol. 17, no. 2, pp. 1038–1052, Feb. 2018, doi: [10.1109/TWC.2017.2773532](https://doi.org/10.1109/TWC.2017.2773532).
- [9] M. F. De Guzman, K. Haneda, and P. Kyösti, "Measurement-based MIMO channel model at 140 GHz (V1)," *Zenodo*, Feb. 2023. [Online]. Available: <https://zenodo.org/records/7640353>
- [10] P. Kyösti, P. Zhang, A. Pärssinen, K. Haneda, P. Koivumäki, and W. Fan, "On the feasibility of out-of-band spatial channel information for millimeter-wave beam search," *IEEE Trans. Antennas Propag.*, vol. 71, no. 5, pp. 4433–4443, May 2023, doi: [10.1109/TAP.2023.3249837](https://doi.org/10.1109/TAP.2023.3249837).
- [11] J. A. Zhang, X. Huang, Y. J. Guo, J. Yuan, and R. W. Heath, "Multi-beam for joint communication and radar sensing using steerable analog antenna arrays," *IEEE Trans. Veh. Technol.*, vol. 68, no. 1, pp. 671–685, Jan. 2019, doi: [10.1109/TVT.2018.2883796](https://doi.org/10.1109/TVT.2018.2883796).
- [12] C. B. Barneto, S. D. Liyanaarachchi, T. Riihonen, L. Anttila, and M. Valkama, "Multibeam design for joint communication and sensing in 5G new radio networks," in *Proc. IEEE Int. Conf. Commun. (ICC)*, Dublin, Ireland, 2020, pp. 1–6.
- [13] N. Tervo, M. E. Leinonen, J. Aikio, T. Rahkonen, and A. Pärssinen, "Analyzing the effects of PA variations on the performance of phased array digital predistortion," in *Proc. IEEE 29th Int. Symp. Pers. Indoor Mobile Radio Commun. (PIMRC)*, Bologna, Italy, Sep. 2018, pp. 215–219, doi: [10.1109/ICC40277.2020.9148935](https://doi.org/10.1109/ICC40277.2020.9148935).
- [14] H. Hammoud et al., "A novel low-cost channel sounder for double-directionally resolved measurements in the mmWave band," *IEEE Trans. Wireless Commun.*, vol. 24, no. 1, pp. 340–354, Jan. 2025, doi: [10.1109/TWC.2024.3492184](https://doi.org/10.1109/TWC.2024.3492184).
- [15] X. Li, X. Cai, E. Leitinger, and F. Tufvesson, "A belief propagation algorithm for multipath-based SLAM with multiple map features: A mmWave MIMO application," in *Proc. IEEE Int. Conf. Commun. Workshops (ICC Workshops)*, Denver, CO, USA, 2024, pp. 269–275.

VT